https://doi.org/10.5194/hess-2020-622
Preprint. Discussion started: 18 December 2020

Hydrology and Earth System Sciences
Discussions
Open Access
EGU

Future projections of High Atlas snowpack and runoff under climate change

Alexandre Tuel[1,4], Nabil El Moçayd[2], Moulay Driss Hasnaoui[3], and Elfatih A. B. Eltahir[1]

[1]Ralph M. Parsons Laboratory, Massachusetts Institute of Technology, 15 Vassar St., Cambridge 02139 USA
[2]International Water Research Institute, University Mohammed VI Polytechnique, Lot 660 Hay Moulay Rachid Benguérir 43150, Morocco
[3]Ministry of Equipement, Transport, Logistics and Water, Department of Water, Morocco
[4]Current affiliation: Institute of Geography, Oeschger Centre for Climate Change Research, University of Bern, Bern

Correspondence: Alexandre Tuel (alexandre.tuel@giub.unibe.ch)

Abstract. The High Atlas, culminating at more than 4000 m, is the water tower of Morocco. While plains receive less than 400 mm of precipitation in an average year, the mountains can get twice as much, often in the form of snow between November and March. Snowmelt thus accounts for a large fraction of the river discharge in the region, and is particularly critical during spring, as the wet season ends but the need for irrigation increases. In the same region, future climate change projections point towards a significant decline in precipitation and enhanced warming of temperature. Understanding how the High Atlas snowpack will evolve under such trends is therefore of paramount importance to make informed projections of future water availability in Morocco. Here, we build on previous research results on snow and climate modeling in the High Atlas to make detailed projections of snowpack and river flow response to climate change in this region. Using a distributed energy balance snow model based on SNOW-17, high-resolution climate simulations over Morocco, and a panel regression framework to relate runoff ratios to regional meteorological conditions, we quantify the severe declines in snowpack and river discharge that are to be expected, even under a scenario of substantial mitigation of emissions. Our results have important implications for water resources planning and sustainability of agriculture in this already water-stressed region.

1 Introduction

The High Atlas is the major source of freshwater for the semi-arid plains of central Morocco. Much of the discharge of the Oum-Er-Rbia and Tensift, the two main rivers of central Morocco, comes from the mountainous terrain where they begin their course. In this region, precipitation essentially falls at elevations above 1000m (Boudhar et al., 2009); below that, it is scarce and evaporation is extremely high, leading to minimal runoff. Though located in a rather warm region, the High Atlas rises up to more than 4000m and often experiences below-freezing conditions between November and March (Boudhar et al., 2009). Consequently, snow is a major component of the regional water cycle (Marchane et al., 2015; Tuel et al., 2020a). It accounts for a substantial fraction of annual runoff, up to 50% in some mountain catchments (Boudhar et al., 2009), and for most of the runoff during spring, as the wet season comes to an end.

Still, climate projections over Morocco happen to agree on robust warming and drying trends under greenhouse gas forcing. By

https://doi.org/10.5194/hess-2020-622
Preprint. Discussion started: 18 December 2020


Hydrology and Earth System Sciences
Discussions

the end of this century, average winter temperatures in the High Atlas could be 2-4°C higher, and precipitation 25-45% lower, depending on the emissions scenario (Tuel et al., 2020b). Being already close to the 0°C isotherm, the High Atlas stands out as particularly vulnerable to snow cover loss. However, few studies have analyzed climate change impacts on the local snowpack and regional water availability. Applying a complex physically-based snow model to one station snow data series from the Moroccan High Atlas, López-Moreno et al. (2017) found that Atlas snowpack was somewhat less sensitive to warming and drying than that in other Mediterranean-climate regions, because of colder snowpack temperatures associated with high latent heat losses. Still, their results pointed to a decrease in average snow duration of 25-30% and in mean Snow Water Equivalent (SWE) of 30-55% by 2050. By contrast, the analysis of 12 years (2000-2013) of remotely-sensed snow cover area from the MODIS satellites yielded few significant trends in snow cover duration across the region (Marchane et al., 2015). At these relatively short timescales, however, the variability in Atlas snow cover is primarily determined by the inter-annual variability in wet-season precipitation, itself largely dependent on the North Atlantic Oscillation (Knippertz et al., 2003; Boudhar et al., 2009). Because precipitation exhibits a large coefficient of annual variation (0.25), potential long-term climate trends will be difficult to identify in such short-term series. Only one study tried to quantify the impact of climate change on High Atlas runoff by taking snow dynamics into account: Marchane et al. (2017) developed runoff projections for the Rheyara catchment, south of Marrakech and part of the Tensift watershed, by running conceptual monthly water-balance models incorporating a simple parametric snow module. They projected a 19 to 63% decline in surface runoff by the middle of the century, dependent on model and scenario. Therefore, while it is clear that the region is headed towards a pronounced decline in snowpack and runoff, much remains to be done to quantify that decline at the catchment level and reduce uncertainties.

Recent work has shed light on the High Atlas snow water balance by applying a simple distributed snow model to reconstruct snowpack within the Oum-Er-Rbia watershed. Tuel et al. (2020a) (hereafter T20a) assimilated remotely-sensed and dynamically-downscaled data into a simple distributed snow model to reconstruct snowpack within the Oum-Er-Rbia watershed and quantify total snow water content and sublimation losses. Here, we build on this methodology by applying the same snow modeling framework to the regional climate projections over Morocco developed by Tuel et al. (2020b) to assess the future of High Atlas snowpack under anthropogenic warming. In addition, we quantify the sensitivity of runoff in seven mountain catchments within the Oum-Er-Rbia watershed to large-scale meteorological conditions, and use the results to assess the impact of warming, drying and snowpack disappearance on runoff. The paper is structured as follows. Section 2 describes the study area, the data and climate model output used in this study. Section 3 presents the snow model and panel regression framework used to model runoff response to large-scale climate conditions. Snowpack and runoff projections are presented and discussed in Section 4. Finally, major results and implications are summarized in Section 6.

2 Study area and data

2.1 Study area

With a length of 550 km, the Oum-Er-Rbia is Morocco's second longest river. There are about 4 km^3 of available renewable water resources in its basin each year, most of which comes from surface runoff (3.5 km^3), the rest being groundwater. 90% of

https://doi.org/10.5194/hess-2020-622
Preprint. Discussion started: 18 December 2020


Hydrology and Earth System Sciences
Discussions

this water is used to irrigate 350000 hectares of fields, accounting for 30% of Morocco's irrigated land, with the rest supporting the needs of two major cities, Casablanca and Marrakech, and industrial phosphate mining. In addition, mountain runoff is used to generate hydroelectricity. The Oum-Er-Rbia river begins its course on the southern slopes of the Middle Atlas, northeast of the city of Khenifra; as it flows westwards towards the Atlantic Ocean, it receives major contributions from northward-flowing tributaries originating in the High Atlas (Fig. 1-a). Beyond that, the river continues its course in semi-arid plains which bring little additional runoff.

The annual cycle of temperature has a large amplitude (Knippertz et al., 2003). Minimum temperatures occur in January, and range from -5°C at high altitudes to 12°C in the plains. Temperatures reach their peak in July, at about 35°C below 1000m and 10-15°C above 3000m (Ouatiki et al., 2017). Precipitation is sparse, even at high altitudes, with an average of about 400mm for the whole basin. The lowest values are found in the lowland plains, at about 250mm annually, while the mountains to the south typically receive up to 800mm (Ouatiki et al., 2017). Most of that precipitation occurs between October and May, when the region is under the influence of North Atlantic westerlies (Knippertz et al., 2003; Tuel and Eltahir, 2018) (Fig. 1-b). Mountainous areas also experience substantial precipitation during summer, due to small-scale convection (Born et al., 2008). As a consequence, vegetation outside the lower-elevation valleys is sparse, essentially limited to bare soil, grass and occasional shrubs (Baba et al. 2019). Snowfall is common between November and March above 1500m elevation, and a somewhat persistent snowpack is not uncommon above 2500m (Marchane et al., 2015). Inter-annual variability is substantial, however, following that of precipitation (Boudhar et al., 2010). Melt is rapid, beginning in March and typically lasting 1-2 months at most (Tuel et al., 2020a).

2.2 Hydroclimatological data

We use for this study a mixture of model-, station- and satellite-based hydrometeorological data. Model-based data is described in section 2.3. Daily precipitation data are available at seven stations in the study area, including three at more than 1200m elevation, over the 1980-2015 period (Fig. 1-a). For each station, we discard the months for which more than 10% of the data is missing. Daily discharge measurements are available at seven locations as well, between 1978 and 2015. Each has at most 0.5% of missing data. These locations define seven sub-catchments for which runoff will be modeled, from north to south: Tarhat, Chacha, Ouchene, Tillouguite, Moulay Hassan, Segmine and Tamesmate (Fig. 1-a). These sub-catchments include most of the area within the Oum-Er-Rbia watershed that receives significant snowfall (Marchane et al., 2015). Their average elevation varies from 1460 to 2360m. We remove the contribution from base flow by subtracting the minimum monthly discharge value for each catchment and each hydrological year (September-August). This correction is minor for all catchments except Tarhat, the northernmost one, which includes the headwaters of the Oum-Er-Rbia river, and receives a substantial contribution of base flow to its annual discharge. In particular, the flow at Tarhat remains high during summer (≈35% of its wet-season peak), likely due to groundwater discharge from deep mountain aquifers. Annual cycles of corrected monthly discharge are shown on Fig. 2-a.

Satellite-based data is used for basin-wide precipitation, temperature and snow cover. 3-hourly precipitation from the TRMM TMPA (TRMM Multi-Satellite Precipitation Analysis) 3B42 version 7 dataset is used as the reference precipitation dataset for

https://doi.org/10.5194/hess-2020-622
Preprint. Discussion started: 18 December 2020


Hydrology and Earth System Sciences
Discussions

the region. It consists in remotely-sensed data corrected with rain gauge data on a monthly basis (Huffman et al., 2007). The data cover the period 1998 to present. While satellite-based precipitation data suffers from numerous biases (Milewski et al., 2015; Derin et al., 2016; Hashemi et al., 2017), it is often the only option available in complex terrain where stations are scarce. Milewski et al. (2015) and Ouatiki et al. (2017) assessed the accuracy of the TRMM 3B42 V7 dataset in the Oum-Er-Rbia and found that, although unreliable at the daily timescale, it offered satisfactory estimates of precipitation if averaged in space or time. Annual cycles of TRMM precipitation for the seven catchments are shown on Fig.1-b.

For comparison, we also consider the CHIRPS dataset, available from 1981 onwards at a 0.05° resolution (Funk 2015). CHIRPS is produced by combining high-resolution satellite-based precipitation with station and fine-scale topography data. In our region of focus, TRMM and CHIRPS show some differences (Fig. 3-a,b): CHIRPS is notably wetter, particularly near the Tizi N'isly station. A comparison of monthly values with the four available stations above 1000m suggests a rather dry bias in TRMM and inconsistent biases in CHIRPS (Fig. 3-c,d). Both datasets have a dry bias over the north-eastern corner of our domain (around the Kenifra station). Across the four stations shown on Fig. 3, absolute biases range from 13.4mm to 25.6mm for TRMM and from 18.6mm to 25.2mm for CHIRPS. Our purpose here is not to perform an in-depth comparison of the performance of the two datasets, but to test the robustness of the runoff projection results to variability in reference precipitation. To bias-correct regional climate model output for snow modeling (Section 3.1), however, we follow T20a and consider only the TRMM dataset. Reference surface air temperature is derived from MODIS Land Surface Temperature (LST) product MOD11A1 L3 version 6 at 1km resolution (Wan, Z., Hook, S., Hulley, 2015). We refer to T20a for details on data filling and correction. Observed snow cover area for the region is extracted from the MODIS Terra snow cover daily L3 product (MOD10A1) at 500m resolution (Hall and Riggs, 2016). Snow cover is detected using values of the Normalized-Difference Snow Index, based on reflectances in the visible/near infrared and middle infrared. We apply the correction methodology described in Marchane et al. (2015) which allows to substantially reduce the number of missing data points due, mainly, to cloud cover, and average the data at the weekly timescale as in T20a. We refer to these two studies for a discussion of the accuracy of the MODIS dataset in this region. All MODIS data is available from February 2000 to present. Elevation data is taken from the Shuttle Radar Topography Mission 90-meter resolution dataset version 4.1 (STRM90) (Jarvis et al., 2008), and interpolated to the approximately 1km resolution of the MODIS land surface temperature data.

2.3 Regional climate simulations

We consider the regional climate downscaling data and projections developed by Tuel et a. (2020b) for the Western Mediterranean, at a 12km resolution, using the MIT Regional Climate Model (MRCM). MRCM is based on the Abdus Salam International Centre for Theoretical Physics Regional Climate Model Version 3 (RegCM3) (Pal et al., 2007), but with significant enhancements of model physics, and notably a coupling with the Integrated BIosphere Simulator land surface scheme (IBIS). Dynamical downscaling is performed for ERA-Interim (1982-2011) (Dee et al., 2011) as well as three carefully-selected GCMs from the Coupled Model Inter-comparison Project Phase 5 (CMIP5) (Taylor et al., 2012): MPI-ESM-MR, GFDL-ESM2M and IPSL-CM5A-LR, for the historical (1976-2005) and RCP4.5 and 8.5 (2071-2100) scenarios. Details of the simulations, including model setup and performance, can be found in Tuel et al. (2020b).

https://doi.org/10.5194/hess-2020-622
Preprint. Discussion started: 18 December 2020


Hydrology and Earth System Sciences
Discussions

6-hourly wind speed, specific humidity, air temperature, precipitation, and downward longwave and shortwave are extracted from the MRCM output over our domain. For all three GCM-driven simulations, as well as the ERA-Interim driven run (hereafter referred to as ERA/MRCM), air temperature and precipitation data are statistically downscaled and bias-corrected at the 6-hourly timescale using MODIS LST-derived air temperature and TRMM precipitation at their native resolutions as respective targets, via the CDF-transform method (Michelangeli et al., 2009). Alone among the three GCMs, the IPSL-CM5A-LR model exhibits a negative bias in wet days that we correct at each grid cell by randomly generating wet days of magnitude drawn from the corresponding distribution of wet-day precipitation in the TRMM dataset. For bias correction, reference periods for ?perfect? observations are 1998-2011 for TRMM and 2000-2011 for MODIS. The corresponding periods in the simulations are the same for ERA/MRCM, and the 1992-2005 and 1994-2005 periods, respectively, for each of the GCM-driven simulations. All bias corrections are performed for the cold (November-April) and warm (May-October) seasons separately.

Additionally, we use wind speed, downward long- and shortwave radiation and specific humidity from the ERA/MRCM simulation over the 1982-2005 period as reference, since no observations are available. The corresponding variables in each GCM-driven simulation are therefore bias-corrected using the ERA/MRCM data as target. Specific humidity is further downscaled to the 1km MODIS LST resolution based on an empirical lapse-rate μ estimated at each time step:

$$\log(q) = \log(q_{12}) + \mu \cdot (z - z_{12}) \tag{1}$$

where q_{12} is the specific humidity in a given 12-km resolution grid cell of elevation z_{12}, and q the downscaled value at elevation z.

3 Methods

The methodological framework adopted in this study is summarized in Fig. 4. We start from GCM simulations from the CMIP5 archive, dynamically-downscaled with MRCM. We apply bias-correction to the MRCM output, which we then feed into a 1km-resolution snow model over our study region to reconstruct snowpack under the various emissions scenarios. Finally, a statistical model is developed for catchment runoff coefficients (RCs), in order to make projections of runoff under future climate conditions.

3.1 Snow model

We apply the SNOW-17 model (Anderson, 2006) with a radiation-derived temperature index for melt (Follum et al., 2015) as described in T20a. SNOW-17 simulates snow accumulation and loss based on meteorological variables, and accounts for the various energy balance equation terms. Snowpack is characterized by its snow water content (SWE) and heat deficit, defined as the amount of heat (in equivalent mm of SWE) required to bring its temperature up to freezing point. We also integrate the bulk-aerodynamic formulation of sublimation detailed in T20a. Readers are referred to Follum et al. (2015) and Anderson (2006) for more details about SNOW-17.

https://doi.org/10.5194/hess-2020-622
Preprint. Discussion started: 18 December 2020


Hydrology and Earth System Sciences
Discussions

We run the model at a 6-hourly time step and at the native MODIS LST 1km resolution over the same 13104 km^2 domain as T20a, that encompasses the seven catchments shown on Fig. 1-a. Elevation in this domain ranges from 621m to 3890m, with an average of 1882m. SWE given by the model is then translated into snow cover fraction for each grid cell using the following relationship:

$$SC = 0.8 \times \tanh\left(k \cdot SWE\right) \tag{2}$$

with $k = 100$. The snow model requires optimizing three parameters: M_f (melt factor), NMF_{max} (maximum negative melt factor) and $TIPM$ (coefficient used in updating snowpack temperature) (Anderson, 2006). In keeping with T20a, parameter calibration is performed by maximizing the Nash-Sutcliffe coefficient (Nash and Sutcliffe, 1970) between the annual cycles of observed (MODIS) and simulated snow cover at 250 randomly selected grid points within the snow domain. We force the elevation distribution of these 250 points to match that of the whole domain. The annual cycles are computed for the 1995-2005 period in the GCM-driven simulations, 2000-2011 period in the ERA-Interim simulation and 2000-2011 period in the MODIS series. Parameter are calibrated independently for each of the simulations (ERA-Interim and three GCMs) in their respective reference periods. For the future simulations, parameter values are kept constant, equal to their calibrated values.

3.2 Statistical modeling of runoff coefficients

We model catchment runoff coefficients (RCs), defined as total October-May discharge divided by total October-May precipitation, across time and space as functions of large-scale hydrological variables by adopting a panel regression framework. Panel regression allows to enhance the effective size of a dataset and to obtain more robust estimates of the response to selected covariates compared to more traditional regression approaches (Steinschneider et al., 2013; Davenport et al., 2020). It also allows to account for static (space-dependent) and time-varying (time-dependent) factors, although here, with only seven catchments, we do not have enough data to make robust statements about static factors responsible for the disparity in average RC (Fig. 2-b). Therefore, we focus on time-varying covariates, and consider a fixed-effects formulation:

$$\log\left(RC_{j,t}\right) = \log\left(\overline{RC}_j\right) + \sum_i \beta_i X^i_{j,t} + \epsilon_{j,t} \tag{3}$$

where $j \in \{1, ..., 7\}$ is the catchment index, t is the time index, i is the covariate index, and $\overline{RC}_j$ represents time-invariant, watershed-specific fixed effects (drainage area, land cover, mean climate), $X^i_{j,t}$ are the covariates, β_i are regression coefficients and $\epsilon_{j,t}$ is random noise. For covariates, we consider catchment-averaged October-May precipitation (P), relative humidity (RH), temperature (T), snow water equivalent (SWE) and snow fraction of precipitation (SF). Enhanced precipitation or relative humidity lead to wetter soils and can be expected to be associated with higher RC values. Similarly, higher temperatures increase evapotranspiration and tend to decrease runoff. Finally, increased snow cover favors losses by sublimation and shifts the distribution of runoff regimes towards slower runoff as opposed to rapid overland flow following rain storms. However,

https://doi.org/10.5194/hess-2020-622
Preprint. Discussion started: 18 December 2020


Hydrology and Earth System Sciences
Discussions

larger snow cover may also increase the risk of rain-over-ice events, which tend to have very high runoff coefficients (Davenport et al., 2020).

Environmental model covariates are calculated using the ERA/MRCM run and associated snow model output, with temperature and precipitation bias-corrected as described previously. While we rely on TRMM as the best gridded daily precipitation dataset available for our area, its main drawback is that it covers only the post-1998 period. Using TRMM directly would limit our analysis to a mere 18 years (1998-2015), likely insufficient given the region's high inter-annual variability in precipitation. Therefore, we use the ERA/MRCM precipitation data, bias-corrected with TRMM, to estimate catchment-scale precipitation for the longer 1982-2011 period, during which runoff data are available for all catchments. This allows us to calculate catchment runoff coefficients (RCs), defined as observed total October-June discharge divided by estimated total October-June precipitation. To assess the robustness of the results, we also calculate RCs based on CHIRPS precipitation (available from 1981-present).

Model selection is performed by stepwise regression: starting from a model with no covariates, covariates are added one at a time in the order of highest improvement to model skill, as determined by its Akaike Information Criterion (AIC). At each step, we also test whether removing any of the currently selected variables and replacing it by one of the remaining, non-selected ones, brings any improvement. To estimate the sensitivity of RC to changes in climate conditions, we modify covariate values in the 1982-2011 ERA-Interim downscaled simulation by adding projected long-term changes in the GCM-driven simulations:

$$\log\left(\widehat{RC}^{m}_{j,t}\right) = \log\left(\overline{RC}_{j}\right) + \sum_{i\in\mathcal{I}} \beta_i \left(X^{i}_{j,t} + \overline{X}^{i}_{m}\right) \tag{4}$$

where $m \in \{1,2,3\}$ is model index, $\mathcal{I}$ is the set of optimal covariates, $X^{i}_{j,t}$ are ERA-Interim downscaled covariate values and $\overline{X}^{i}_{m}$ represent long-term covariate changes drawn at random according to:

$$\overline{X}^{i}_{m} \sim N\left(\mu^{i}_{m,\mathrm{rcp}} - \mu^{i}_{m,\mathrm{hist}}, \sqrt{\sigma^{i}_{m,\mathrm{rcp}} + \sigma^{i}_{m,\mathrm{hist}}}\right) \tag{5}$$

where $\mu^{i}_{m,s}$ (respectively $\sigma^{i}_{m,s}$ is the average (respectively standard deviation) of covariate i in model m and scenario s. Results for the three models are then pooled together to yield a future distribution for $RC_{j,t}$.

4 Results and discussion

4.1 Snowpack projections

Annual cycles of reconstructed snow cover as a function of elevation are shown on Fig. 5. Overall, all models succeed in accurately reproducing snow cover dynamics in the region, although the ERA-Interim simulation tends to have a positive bias at high elevations, particularly above 3000m (Fig. 5-b) and all simulations have a negative bias at low elevations (Figs. 5-d,e and 6-a,b). The GCM-driven experiments generally show too little snow cover, and a later snowpack build-up (Fig. 5-f).

https://doi.org/10.5194/hess-2020-622
Preprint. Discussion started: 18 December 2020


Hydrology and Earth System Sciences
Discussions

December-March average snow cover over the whole modeled area reaches 1460 km2 in MODIS observations but only 1275 km^2 in the ERA-Interim driven run and 1185 km^2 in the ensemble mean historical average – a bias largely concentrated at low elevations. Additionally, despite the statistical downscaling of the MRCM output to 1km, elevation-driven gradients in snow cover are also less sharp in the MRCM experiments compared to observations (Fig. 6-a,b). All results tend to remain however in a narrow band around the MODIS values and, except for elevations below 2000m, inter-model spread generally covers observed snow cover values. Inter-annual variability in basin-wide snow cover is lower in the simulations compared to MODIS (standard deviation of 220-440 km^2 compared to 480 km^2 in MODIS) but the discrepancy is mainly due to the negative bias at low elevations, where snow plays a much more limited role in the overall water balance (T20a). Unsurprisingly, future projections show a stark decline in snow cover across all the region (Figs. 6, 7). The greatest relative decline is at low elevations, as expected since they are already seldom above the 0°C line (Boudhar et al., 2016). Above 2500m, projections still exhibit a 30-40% decrease in snow cover area under RCP4.5 and 50-60% decrease under RCP8.5. Projected trends are even steeper in terms of snowpack water content (Fig. 8): it is reduced on average by 60% under RCP4.5 and 80-85% under RCP8.5, bringing peak SWE value from about 125 million m^3 (MCM) down to 20 MCM (Figs. 8-f, 9). The corresponding projected wet-season precipitation declines are about 25% under RCP4.5 and 40-45% under RCP8.5 (Tuel et al., 2020b). Because most areas in the High Atlas are very close to the zero-degree line, even at high elevations, warming trends largely amplify the precipitation signal and result in larger relative SWE declines. Warming causes the percentage of solid precipitation to decrease, particularly at mid-elevations (2000-2500m) (Fig. 10) and also favors melt during winter, thus preventing the build-up of the snowpack.

As discussed in T20a, the historical SWE peak of 125 MCM is subject to caution; experiments with enhanced precipitation or reduced temperatures suggest it may in fact be as high as 200 MCM. Still, while inter-model spread is large in the historical experiments (≈60MCM) and still large (≈40MCM) in the RCP4.5 experiment, it is reduced to almost zero under RCP8.5. Whatever the historical disparity in temperatures or precipitation between models, all models agree on the quasi-absence of snowpack under business-as-usual. This is consistent with observations that in mountain regions, above-freezing temperatures are common, even at high altitudes, where average winter temperatures are not far from freezing (López-Moreno et al., 2017). Therefore, under the RCP8.5 scenario, the projected 4°C warming (Tuel et al. 2020b) would regularly bring all areas but the very highest peaks well above freezing, and prevent seasonal snowpack accumulation.

Due to the particularly arid climate of the High Atlas, sublimation losses are quite significant in our study area: about 9% of all snowfall on average, and up to 30% above 3500m (Schulz and de Jong (2004); López-Moreno et al. (2017),T20a). Annual relative sublimation losses are strongly linked to annual-mean precipitation (Fig. 11-a). Losses from latent heat fluxes are much smaller during wet years as compared to dry years, a relationship robust across all experiments. Wet years indeed bring higher RH over the region, due to enhanced moisture advection from the Atlantic which more than compensates for the larger heat advection and increased air temperatures that also occur in parallel (Knippertz et al., 2003). In addition to higher RH limiting evaporation and increasing soil moisture, warmer temperatures in wetter years also tend to decrease the snow-to-precipitation ratio, thus leading to reduced relative sublimation losses. Consequently, we expect the runoff coefficient to be higher in wet years. Under future climate conditions, average relative humidity will decline by 3-6% (Tuel et al., 2020b), and thus sublimation rates will be higher when snow is present. However, because the snow-to-precipitation ratio will also sharply

https://doi.org/10.5194/hess-2020-622
Preprint. Discussion started: 18 December 2020


Hydrology and Earth System Sciences
Discussions

decline due to rising temperatures, the overall loss of annual precipitation by sublimation will tend to decrease by about a third (Fig. 11-b).

For the areas as a whole, decreasing precipitation and warmer temperatures are the primary causes of the projected decline in snowpack. In addition, drier soils together with enhanced absorption of solar energy where snowpack disappears will also lead to enhanced warming locally, driving yet further snowpack melt. We do not explicitly take this into account in our model. In particular, the snow albedo effect is largely absent from the MRCM simulations due to their 12km resolution, which is still too coarse to represent the complex topography. For areas at the highest elevations (near 4000m) which may still remain largely below freezing in future winters, melt may not increase very significantly in the middle of winter; however, a drier atmosphere will still be associated with reduced precipitation and increased sublimation losses, which will play a critical role in reducing the snowpack.

4.2 Runoff modeling and projections

The panel regression and model selection framework are applied to runoff coefficients and selected covariates over the 1982-2011 period. Stepwise regression yields as optimal covariates relative humidity and snow fraction. The adjusted r^2 is equal to 0.30, meaning that these two covariates explain a small third of inter-annual variability in RC. Fitted RCs against observations are shown on Fig. 12. Consistent with the model r^2, fitted values have a much smaller variance. Still, for all the catchments, except Segmine, we observe a significant positive relationship between fitted and observed values. The coefficients for RH and snow fraction are both significant, with $\beta_{RH} > 0$ and $\beta_{SF} < 0$ (Table 1). All else being equal, a larger RH yields more runoff – consistent with previous studies (Wang et al., 2016; Duan et al., 2017) – and more of the precipitation falling as snow yields less runoff. These results are robust to the choice of the precipitation dataset. When using the CHIRPS dataset, average RCs are generally lower, due to CHIRPS?s wet bias compared to TRMM (Fig. 3); the optimal RC model includes RH and SF as well, but also precipitation as a third variable (Table 1). The values of β_{RH} and β_{SF} obtained with CHIRPS data are similar, although β_{SF} is slightly less significant.

For both precipitation datasets, the effect of RH on runoff coefficient, as measured by the respective regression coefficient β_{RH}, is 3-5 times that of snow. As discussed above, we can understand the influence of snow fraction by noting that a higher snow fraction means more opportunity for sublimation, particularly large at high elevations, and evaporation of melted snow, consistent with our analysis of sublimation losses (Fig. 11). Precipitation in the area tend to occur in short and intense storms, and quickly saturate the dry soil, leading to rapid overland flow with limited opportunity for evaporation (El Khalki et al., 2018). By comparison, snowmelt is slow and leads to a more gradual surface flow with the potential for higher evaporative losses in this climate where evaporation tends to be water-limited. More winter snow also leads to a higher likelihood of rain-on-snow episodes in spring, known to cause rapid flooding due to high runoff efficiencies (Davenport et al., 2020). More snow may also mean more opportunity for infiltration and aquifer recharge (Hssaisoune et al., 2020); however, in six out of seven catchments considered here, base flow is negligible. Still, aquifer discharge may occur naturally further down the mountains, or artificially via direct groundwater pumping in the agricultural plains. Compared to surface runoff, groundwater remains a small fraction of water use in the Oum-Er-Rbia basin ($<$15%), and even less of available renewable water since aquifers are

https://doi.org/10.5194/hess-2020-622
Preprint. Discussion started: 18 December 2020


Hydrology and Earth System Sciences
Discussions

largely overdrawn (Hssaisoune et al., 2020). Groundwater data are quite scarce in this region; we make the choice of purely focusing on surface runoff, keeping in mind that a more complete picture of basin-wide water availability would also require taking aquifer fluxes into account.

Future runoff projections are characterized by consistent, steep declines in runoff coefficients of 5-17% under RCP4.5 and 15-30% under RCP8.5 (Fig. 13-a). The impact of decreasing RH largely dominates over that of declining snow fraction. Tarhat and Chacha, the two watersheds which already receive almost no snow in the present climate, exhibit the greatest relative RC decline, whereas in other watersheds, decreases in snow fraction help limit the decline in RC (Table 2). Combining now precipitation and runoff coefficient estimates, we find a 20-40% decrease in runoff in the RCP4.5 experiments, compared to a 50-65% decline under RCP8.5 (Fig. 13-b, Table 2). Decreases in precipitation drive most of the runoff trends, especially in the RCP8.5 scenario. Projected RC declines are about the same when using CHIRPS data for the analysis, although tend to be slightly higher, on average by 3-6% on average (not shown). Our projected runoff trends are consistent with those of El Moçayd et al. (2020) who focused on catchments part of the Sebou watershed, where snow plays a much smaller role than in our region (Marchane et al., 2015). This is not surprising given the weak impact of the declining snow fraction on runoff coefficients, compared to that of the relative humidity decline. As a final note, one can ask whether observed runoff trends are consistent with these projections. At the country scale, government data indicates that river discharge has indeed significantly declined over the last 60 to 70 years, at a rate of about 5% per decade (Fig. A1). The wet years of the 1960s tend however to bias the result towards a steeper decline than expected. In this case, natural decadal variability linked to the North Atlantic Oscillation acted in the same direction as the expected climate change response. Runoff data from the seven sub-catchments studied here are less clear. They cover shorter time periods (by about 25 years) and, more importantly, begin in the late 1970s, just when the climate turned much drier in Morocco; drier-than-average conditions indeed prevailed from 1980 to the mid-1990s, associated with increased frequency in the positive phase of the North Atlantic Oscillation. Thus, runoff trends tend to be slightly positive (about +1%/yr), though none are significant, even at the 10% level.

5 Conclusions

Based on the robust understanding of its snow water balance in the current climate, we quantified in this final chapter the response of the High Atlas snowpack to climate change using high-resolution downscaled climate projections. Unsurprisingly, given the warming and drying trends projected by climate models for this region, we find that the High Atlas snowpack will significantly decline, even with substantial mitigation of emissions. By the end of the century, snow may become a rarity below 2000m, and even near the highest peaks, snowpack water equivalent could decline by 80%. Precipitation decreases of 40-60% are responsible for much of these trends, with background warming accounting for the rest.

The analysis of runoff coefficients for seven mountain catchments showed that a third of their inter-annual variability could be explained by large-scale meteorological factors like snow fraction of precipitation and relative humidity. Interestingly, in this region, a larger snow fraction leads to less runoff. While the reverse is believed to be true at higher latitudes (Berghuijs et al., 2014), this finding is consistent with other analyses in warm, semi-arid regions that receive substantial amounts of snow

https://doi.org/10.5194/hess-2020-622
Preprint. Discussion started: 18 December 2020


Hydrology and Earth System Sciences
Discussions

during winter (Davenport et al., 2020). Warmer conditions tend to enhance runoff efficiencies by reducing snowpack, thus limiting sublimation losses and the slow melting of snow, propitious to evaporation, and by increasing the likelihood of rain-on-snow events that tend to cause high runoff efficiencies. While decreasing snowfall will partly compensate for the projected atmospheric drying over the region, runoff coefficients will tend to decline by 5-30% depending on catchment and scenario. Combined with precipitation trends, basin-wide runoff could be reduced by 60% in the worst case. In addition, earlier snowmelt will likely lead to lower soil moisture levels during spring, further enhancing the temperature rise and increasing the risk of late-season droughts.

The robust physical understanding behind large-scale projections for the region (Tuel and Eltahir, 2020) increases the likelihood that the dire projections detailed above will be realized provided greenhouse gas emissions are not brought under control. This would deal a severe blow to the region, jeopardizing its agriculture-based economy and the livelihood of millions of smallholder farmers. Agriculture, which accounts for 90% of current water use, will have no choice but to adapt. A 40-60% precipitation decline would make rainfed agriculture infeasible. At the same time, availability of water for irrigation will also decline sharply. A change of cropping patterns, like a transition to tree crops with less water demand and higher economic value like olives, will likely be unavoidable for Morocco to adapt to this future reality.

Data availability. The data used in this study are available from the corresponding author upon request.

Appendix A: Appendix

A1 Supplementary figure A1

Author contributions. EABE conceived and supervised the study. AT carried out analyses and wrote the first manuscript draft. NEM and MDH contributed with data and interpretation of results. All authors contributed to editing the manuscript.

Competing interests. The authors declare that they have no competing financial interests.

Acknowledgements. This work was funded by the Office Chérifien des Phosphates (OCP) through Université Mohamed VI Polytechnique, Morocco. The authors would like to thank Michael Follum and Jeffrey Niemann for providing their RTI-SNOW-17 code.

https://doi.org/10.5194/hess-2020-622
Preprint. Discussion started: 18 December 2020

Hydrology and Earth System Sciences
Discussions

References

Anderson, E. A.: Snow Accumulation and Ablation Model - SNOW-17, Tech. Rep. User Documentation, U.S. National Weather Service, Silver Springs, MD, 2006.

Berghuijs, W. R., Woods, R. A., and Hrachowitz, M.: A precipitation shift from snow towards rain leads to a decrease in streamflow, Nature Climate Change, 4, 583–586, https://doi.org/10.1038/nclimate2246, http://www.nature.com/articles/nclimate2246, 2014.

Born, K., Fink, A. H., and Paeth, H.: Dry and wet periods in the northwestern Maghreb for present day and future climate conditions, Meteorologische Zeitschrift, 17, 533–551, https://doi.org/10.1127/0941-2948/2008/0313, 2008.

Boudhar, A., Hanich, L., Boulet, G., Duchemin, B., Berjamy, B., and Chehbouni, A.: Evaluation of the Snowmelt Runoff model in the Moroccan High Atlas Mountains using two snow-cover estimates, Hydrological Sciences Journal, 54, 1094–1113, https://doi.org/10.1623/hysj.54.6.1094, 2009.

Boudhar, A., Duchemin, B., Hanich, L., Jarlan, L., Chaponnière, A., Maisongrande, P., Boulet, G., and Chehbouni, A.: Long-term analysis of snow-covered area in the Moroccan High-Atlas through remote sensing, International Journal of Applied Earth Observation and Geoinformation, 12, https://doi.org/10.1016/j.jag.2009.09.008, 2010.

Boudhar, A., Boulet, G., Hanich, L., Sicart, J. E., and Chehbouni, A.: Energy fluxes and melt rate of a seasonal snow cover in the Moroccan High Atlas, Hydrological Sciences Journal, 61, 931–943, https://doi.org/10.1080/02626667.2014.965173, 2016.

Davenport, F. V., Herrera-Estrada, J. E., Burke, M., and Diffenbaugh, N. S.: Flood Size Increases Nonlinearly Across the Western United States in Response to Lower Snow-Precipitation Ratios, Water Resources Research, 56, https://doi.org/10.1029/2019WR025571, https://onlinelibrary.wiley.com/doi/abs/10.1029/2019WR025571, 2020.

Dee, D. P., Uppala, S. M., Simmons, A. J., Berrisford, P., Poli, P., Kobayashi, S., Andrae, U., Balmaseda, M. A., Balsamo, G., Bauer, P., Bechtold, P., Beljaars, A. C., van de Berg, L., Bidlot, J., Bormann, N., Delsol, C., Dragani, R., Fuentes, M., Geer, A. J., Haimberger, L., Healy, S. B., Hersbach, H., Hólm, E. V., Isaksen, L., Kållberg, P., Köhler, M., Matricardi, M., Mcnally, A. P., Monge-Sanz, B. M., Morcrette, J. J., Park, B. K., Peubey, C., de Rosnay, P., Tavolato, C., Thépaut, J. N., and Vitart, F.: The ERA-Interim reanalysis: Configuration and performance of the data assimilation system, Quarterly Journal of the Royal Meteorological Society, 137, 553–597, https://doi.org/10.1002/qj.828, https://doi.org/10.1002/qj.828, 2011.

Derin, Y., Anagnostou, E., Berne, A., Borga, M., Boudevillain, B., Buytaert, W., Chang, C. H., Delrieu, G., Hong, Y., Hsu, Y. C., Lavado-Casimiro, W., Manz, B., Moges, S., Nikolopoulos, E. I., Sahlu, D., Salerno, F., Rodríguez-Sánchez, J. P., Vergara, H. J., and Yilmaz, K. K.: Multiregional satellite precipitation products evaluation over complex terrain, Journal of Hydrometeorology, 17, 1817–1836, https://doi.org/10.1175/JHM-D-15-0197.1, 2016.

Duan, K., Sun, G., McNulty, S. G., Caldwell, P. V., Cohen, E. C., Sun, S., Aldridge, H. D., Zhou, D., Zhang, L., and Zhang, Y.: Future shift of the relative roles of precipitation and temperature in controlling annual runoff in the conterminous United States, Hydrology and Earth System Sciences, 21, 5517–5529, https://doi.org/10.5194/hess-21-5517-2017, https://hess.copernicus.org/articles/21/5517/2017/, 2017.

El Khalki, E. M., Tramblay, Y., El Mehdi Saidi, M., Bouvier, C., Hanich, L., Benrhanem, M., and Alaouri, M.: Comparison of modeling approaches for flood forecasting in the High Atlas Mountains of Morocco, Arabian Journal of Geosciences, 11, 410, https://doi.org/10.1007/s12517-018-3752-7, http://link.springer.com/10.1007/s12517-018-3752-7, 2018.

El Moçayd, N., Kang, S., and Eltahir, E. A.: Climate change impacts on the Water Highway project in Morocco, Hydrology and Earth System Sciences, 24, 1467–1483, https://doi.org/10.5194/hess-24-1467-2020, https://hess.copernicus.org/articles/24/1467/2020/, 2020.

https://doi.org/10.5194/hess-2020-622
Preprint. Discussion started: 18 December 2020

Follum, M. L., Downer, C. W., Niemann, J. D., Roylance, S. M., and Vuyovich, C. M.: A radiation-derived temperature-index snow routine for the GSSHA hydrologic model, Journal of Hydrology, 529, 723–736, https://doi.org/10.1016/j.jhydrol.2015.08.044, 2015.

Hall, D. K. and Riggs, G. A.: MODIS/Terra Snow Cover Daily L3 Global 500m SIN Grid, Version 6. MOD10A1 and MYD10A1, https://doi.org/10.5067/MODIS/MOD10A1.006, https://nsidc.org/data/MOD10A1/versions/6, 2016.

Hashemi, H., Nordin, M., Lakshmi, V., Huffman, G. J., and Knight, R.: Bias correction of long-term satellite monthly precipitation product (TRMM 3B43) over the conterminous United States, Journal of Hydrometeorology, 18, 2491–2509, https://doi.org/10.1175/JHM-D-17-0025.1, 2017.

Hssaisoune, M., Bouchaou, L., Sifeddine, A., Bouimetarhan, I., and Chehbouni, A.: Moroccan groundwater resources and evolution with global climate changes, Geosciences (Switzerland), 10, 81, https://doi.org/10.3390/geosciences10020081, https://www.mdpi.com/2076-3263/10/2/81, 2020.

Huffman, G. J., Adler, R. F., Bolvin, D. T., Gu, G., Nelkin, E. J., Bowman, K. P., Hong, Y., Stocker, E. F., and Wolff, D. B.: The TRMM Multisatellite Precipitation Analysis (TMPA): Quasi-global, multiyear, combined-sensor precipitation estimates at fine scales, Journal of Hydrometeorology, 8, 38–55, https://doi.org/10.1175/JHM560.1, 2007.

Jarvis, A., Nelson, A., and Guevara, E.: Jarvis, A., H.I. Reuter, A. Nelson, E. Guevara, 2008, Hole-filled SRTM for the globe Version 4, available from the CGIAR-CSI SRTM 90m Database (http://srtm.csi.cgiar.org), http://srtm.csi.cgiar.org, 2008.

Knippertz, P., Christoph, M., and Speth, P.: Long-term precipitation variability in Morocco and the link to the large-scale circulation in recent and future climates, Meteorology and Atmospheric Physics, 83, 67–88, https://doi.org/10.1007/s00703-002-0561-y, 2003.

López-Moreno, J. I., Gascoin, S., Herrero, J., Sproles, E. A., Pons, M., Alonso-González, E., Hanich, L., Boudhar, A., Musselman, K. N., Molotch, N. P., Sickman, J., and Pomeroy, J.: Different sensitivities of snowpacks to warming in Mediterranean climate mountain areas, Environmental Research Letters, 12, https://doi.org/10.1088/1748-9326/aa70cb, 2017.

Marchane, A., Jarlan, L., Hanich, L., Boudhar, A., Gascoin, S., Tavernier, A., Filali, N., Le Page, M., Hagolle, O., and Berjamy, B.: Assessment of daily MODIS snow cover products to monitor snow cover dynamics over the Moroccan Atlas mountain range, Remote Sensing of Environment, 160, 72–86, https://doi.org/10.1016/j.rse.2015.01.002, 2015.

Marchane, A., Tramblay, Y., Hanich, L., Ruelland, D., and Jarlan, L.: Climate change impacts on surface water resources in the Rheraya catchment (High Atlas, Morocco), Hydrological Sciences Journal, 62, 979–995, https://doi.org/10.1080/02626667.2017.1283042, https://doi.org/10.1080/02626667.2017.1283042, 2017.

Michelangeli, P. A., Vrac, M., and Loukos, H.: Probabilistic downscaling approaches: Application to wind cumulative distribution functions, Geophysical Research Letters, 36, L11 708, https://doi.org/10.1029/2009GL038401, http://doi.wiley.com/10.1029/2009GL038401, 2009.

Milewski, A., Elkadiri, R., and Durham, M.: Assessment and comparison of TMPA satellite precipitation products in varying climatic and topographic regimes in Morocco, Remote Sensing, 7, 5697–5717, https://doi.org/10.3390/rs70505697, 2015.

Nash, J. E. and Sutcliffe, J. V.: River flow forecasting through conceptual models part I - A discussion of principles, Journal of Hydrology, 10, 282–290, https://doi.org/10.1016/0022-1694(70)90255-6, 1970.

Ouatiki, H., Boudhar, A., Tramblay, Y., Jarlan, L., Benabdelouhab, T., Hanich, L., El Meslouhi, M. R., and Chehbouni, A.: Evaluation of TRMM 3B42 V7 rainfall product over the Oum Er Rbia watershed in Morocco, Climate, 5, https://doi.org/10.3390/cli5010001, 2017.

Pal, J. S., Giorgi, F., Bi, X., Elguindi, N., Solmon, F., Gao, X., Rauscher, S. A., Francisco, R., Zakey, A., Winter, J., Ashfaq, M., Syed, F. S., Bell, J. L., Differbaugh, N. S., Karmacharya, J., Konari, A., Martinez, D., Da Rocha, R. P., Sloan, L. C., and Steiner, A. L.: Regional climate modeling for the developing world: The ICTP RegCM3 and RegCNET, Bulletin of the American Meteo-

rological Society, 88, 1395–1409, https://doi.org/10.1175/BAMS-88-9-1395, https://journals.ametsoc.org/bams/article/88/9/1395/59093/Regional-Climate-Modeling-for-the-Developing-World, 2007.

Schulz, O. and de Jong, C.: Snowmelt and sublimation: Field experiments and modelling in the High Atlas Mountains of Morocco, Hydrology and Earth System Sciences, 8, 1076–1089, https://doi.org/10.5194/hess-8-1076-2004, 2004.

Steinschneider, S., Yang, Y. C. E., and Brown, C.: Panel regression techniques for identifying impacts of anthropogenic landscape change on hydrologic response, Water Resources Research, 49, 7874–7886, https://doi.org/10.1002/2013WR013818, http://doi.wiley.com/10.1002/2013WR013818, 2013.

Taylor, K. E., Stouffer, R. J., and Meehl, G. A.: An overview of CMIP5 and the experiment design, Bulletin of the American Meteorological Society, 93, 485–498, https://doi.org/10.1175/BAMS-D-11-00094.1, 2012.

Tuel, A. and Eltahir, E. A.: Seasonal Precipitation Forecast Over Morocco, Water Resources Research, 54, 9118–9130, https://doi.org/10.1029/2018WR022984, 2018.

Tuel, A. and Eltahir, E. A. B.: Why Is the Mediterranean a Climate Change Hot Spot?, Journal of Climate, 33, 5829–5843, https://doi.org/10.1175/JCLI-D-19-0910.1, http://journals.ametsoc.org/doi/10.1175/JCLI-D-19-0910.1https://journals.ametsoc.org/jcli/article/33/14/5829/347612/Why-Is-the-Mediterranean-a-Climate-Change-Hot-Spot, 2020.

Tuel, A., Chehbouni, A., and A. B. Eltahir, E.: Dynamics of seasonal snowpack over the High Atlas, Journal of Hydrology, p. 125657, https://doi.org/10.1016/j.jhydrol.2020.125657, https://linkinghub.elsevier.com/retrieve/pii/S0022169420311185, 2020a.

Tuel, A., Kang, S., and Eltahir, E. A. B.: Understanding climate change over the southwestern Mediterranean using high-resolution simulations, Climate Dynamics, https://doi.org/10.1007/s00382-020-05516-8, http://link.springer.com/10.1007/s00382-020-05516-8, 2020b.

Wan, Z., Hook, S., Hulley, G.: MOD11A1 MODIS/Terra Land Surface Temperature/Emissivity Daily L3 Global 1km SIN Grid V006. NASA EOSDIS Land Processes DAAC, https://doi.org/10.5067/MODIS/MOD11A1.006, https://doi.org/10.5067/MODIS/MOD11A1.006, 2015.

Wang, W., Zou, S., Shao, Q., Xing, W., Chen, X., Jiao, X., Luo, Y., Yong, B., and Yu, Z.: The analytical derivation of multiple elasticities of runoff to climate change and catchment characteristics alteration, Journal of Hydrology, 541, 1042–1056, https://doi.org/10.1016/j.jhydrol.2016.08.014, http://www.sciencedirect.com/science/article/pii/S0022169416305042, 2016.

https://doi.org/10.5194/hess-2020-622
Preprint. Discussion started: 18 December 2020

Hydrology and Earth System Sciences
Discussions
Open Access
EGU

Table 1. Runoff coefficient model results. The bottom three lines show coefficient values (left-hand column) and their statistical significance (p-value, right-hand column).

	MRCM-BC		**CHIRPS**	
r^2	0.30		0.36	
SF	-1.84	4E-03	-1.47	2E-02
RH	5.71	2E-05	8.71	1E-09
Pr	–	–	2.04E-03	1E-06

https://doi.org/10.5194/hess-2020-622
Preprint. Discussion started: 18 December 2020

Hydrology and Earth System Sciences
Discussions
Open Access
EGU

Table 2. Long-term (2071-2100 minus 1976-2005) projections for the seven catchments: October-May temperature (°C), precipitation (%), relative humidity (%), absolute and relative snow fraction (%), runoff coefficient (%) and runoff (%), under RCP4.5 and RCP8.5.

Catchment	M. Hassan		Tamesmate		Tillouguite		Segmine		Ouchene		Tarhat		Chacha	
	RCP4.5	RCP8.5	RCP4.5	RCP8.5	RCP4.5	RCP8.5	RCP4.5	RCP8.5	RCP4.5	RCP8.5	RCP4.5	RCP8.5	RCP4.5	RCP8.5
$\Delta T(^{\circ}C)$	2.3	4.6	2.2	4.4	2.2	4.5	2.3	4.6	2.3	4.6	2.3	4.8	2.3	4.7
ΔPr (%)	-11	-53	-14	-57	-30	-57	-22	-48	-31	-57	-31	-50	-31	-55
ΔRH (%)	-3.1	-6.2	-2.5	-5.5	-3.2	-6.4	-3.6	-7.1	-3.4	-6.3	-3.2	-6.6	-3.2	-6.1
ΔSnow (%)	-3.3	-11.3	-3.9	-12.3	-6.7	-15.7	-5.7	-14.9	-6	-11.3	-5	-7.5	-2	-3.2
ΔSF (%)	-14	-46	-16	-51	-19	-44	-19	-51	-28	-52	-52	-78	-50	-80
ΔRC (%)	-14	-23	-8	-17	-6	-14	-10	-17	-9	-19	-13	-27	-15	-30
ΔRunoff (%)	-23	-64	-21	-64	-34	-63	-29	-57	-37	-65	-39	-63	-41	-68

https://doi.org/10.5194/hess-2020-622
Preprint. Discussion started: 18 December 2020

Hydrology and Earth System Sciences
Discussions
Open Access
EGU

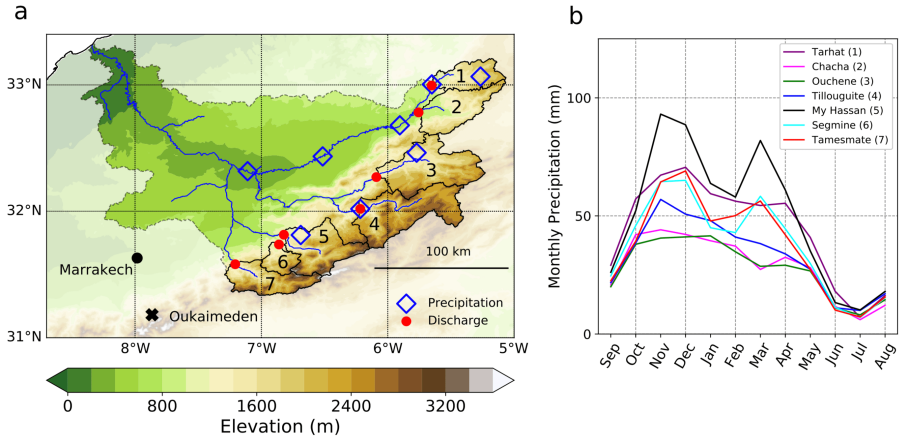

Figure 1. (a) Map of study area, the Oum-Er-Rbia watershed, with elevation shown in filled contours. The main waterways are indicated by solid blue lines. Blue diamonds and red circles indicate the location of precipitation and river discharge stations, respectively. The seven catchments defined by the discharge stations are indicated by numbers: (1) Tarhat, (2) Chacha, (3) Ouchene, (4) Tillouguite, (5) Moulay Hassan, (6) Segmine and (7) Tamesmate. The location of the Oukaimeden snow station, outside our study area, is shown by a black cross. (b) Annual cycles of precipitation for the seven catchments, based on TRMM data (1998-2015).

https://doi.org/10.5194/hess-2020-622
Preprint. Discussion started: 18 December 2020

Hydrology and Earth System Sciences
Discussions
Open Access
EGU

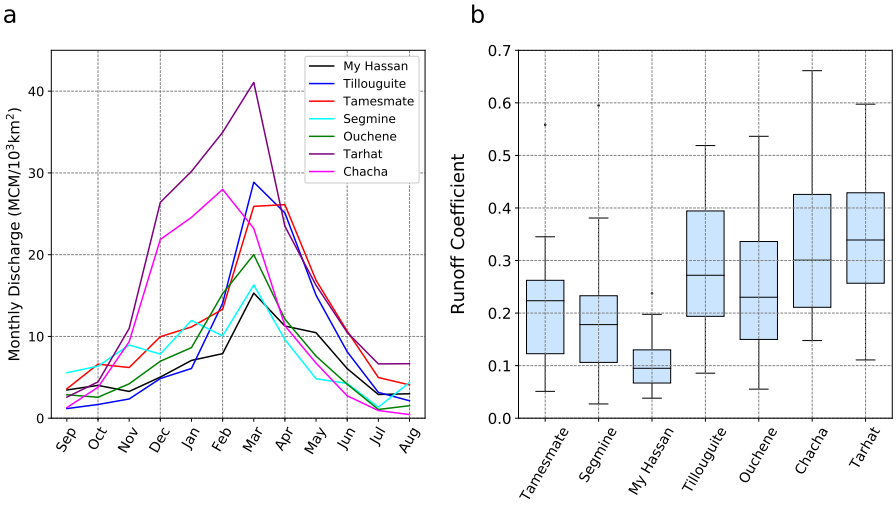

Figure 2. (a) Annual cycles of monthly runoff at the seven runoff gauges, after base flow removal and normalization by catchment area (km2). (b) Boxplot of annual runoff coefficients for the seven catchments (1982-2011), using ERA/MRCM precipitation bias-corrected with TRMM data.

https://doi.org/10.5194/hess-2020-622
Preprint. Discussion started: 18 December 2020

Hydrology and Earth System Sciences
Discussions
Open Access
EGU

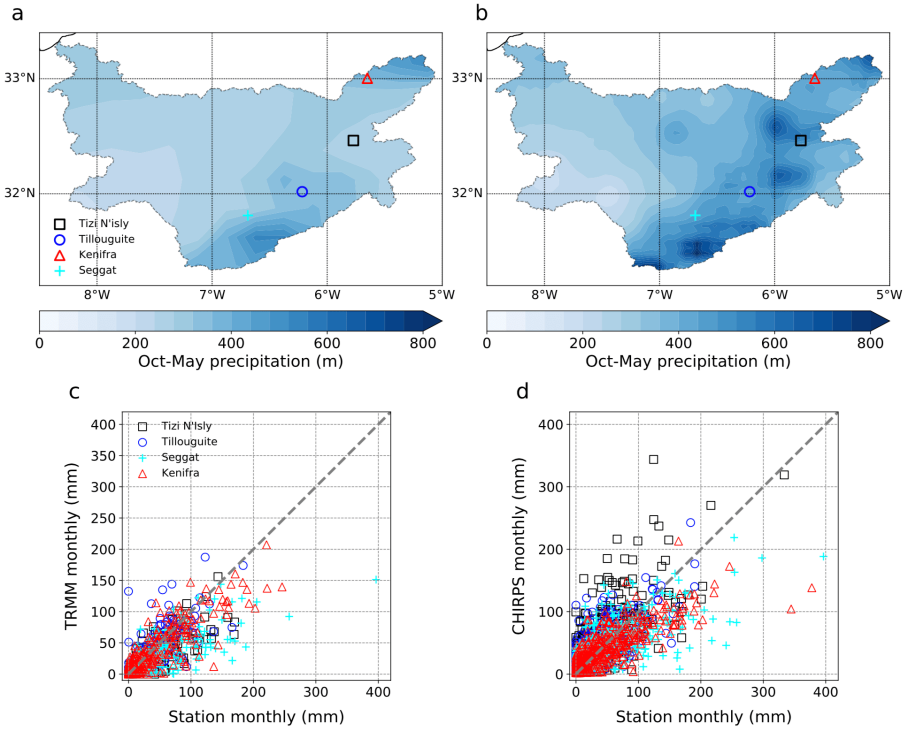

Figure 3. (a) October-May average precipitation (mm) over the Oum-Er-Rbia watershed, from TRMM (1998-2015). The four available precipitation stations above 1000m elevation are indicated by symbols. (c) Monthly precipitation at the four stations shown on (a) against corresponding TRMM values. (b,d) Same as (a,c) but for the CHIRPS dataset (1981-2015).

https://doi.org/10.5194/hess-2020-622
Preprint. Discussion started: 18 December 2020

Hydrology and Earth System Sciences
Discussions
Open Access
EGU

Figure 4. Summary of methodology to assess climate change impacts on snowfall, snowpack and runoff in the Oum-Er-Rbia watershed.

https://doi.org/10.5194/hess-2020-622
Preprint. Discussion started: 18 December 2020

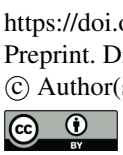

Hydrology and Earth System Sciences
Discussions
Open Access
EGU

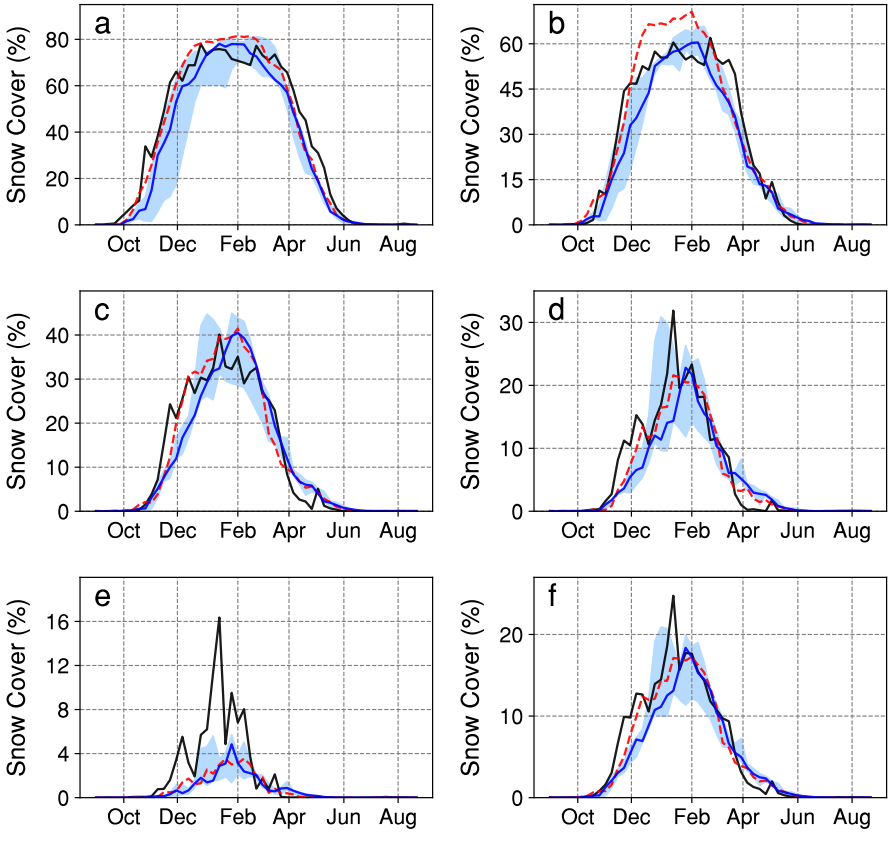

Figure 5. Annual cycles of snow cover (in %) in the MODIS observations (black), ERA- Interim simulation (dashed red) and three GCM-driven historical simulations (solid blue: me- dian; blue shading: 3-model range), at various elevations ranges within our study area: (a) > 3500m, (b) 3000-3500m, (c) 2500-3000m, (d) 2000-2500m, (e) 1500-2000m and (f) whole area.

https://doi.org/10.5194/hess-2020-622
Preprint. Discussion started: 18 December 2020

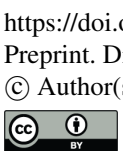

Hydrology and Earth System Sciences
Discussions
Open Access
EGU

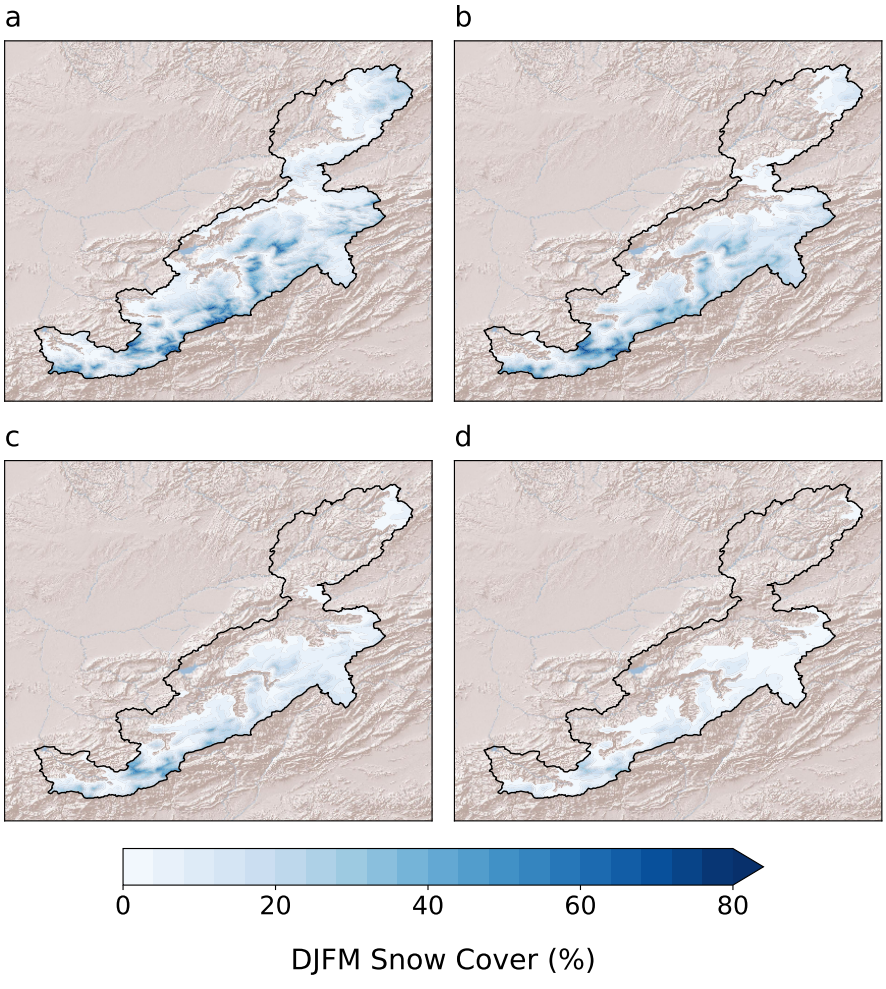

Figure 6. Mean December-to-March (DJFM) fractional snow cover (%) over the basin in (a) MODIS (2000-2010) data, and (b-d) three-GCM average under the (b) historical (1976-2005), (c) RCP4.5 (2071-2100) and (d) RCP8.5 (2071-2100) experiments.

https://doi.org/10.5194/hess-2020-622
Preprint. Discussion started: 18 December 2020

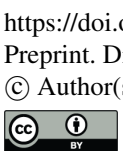

Hydrology and Earth System Sciences
Discussions
Open Access
EGU

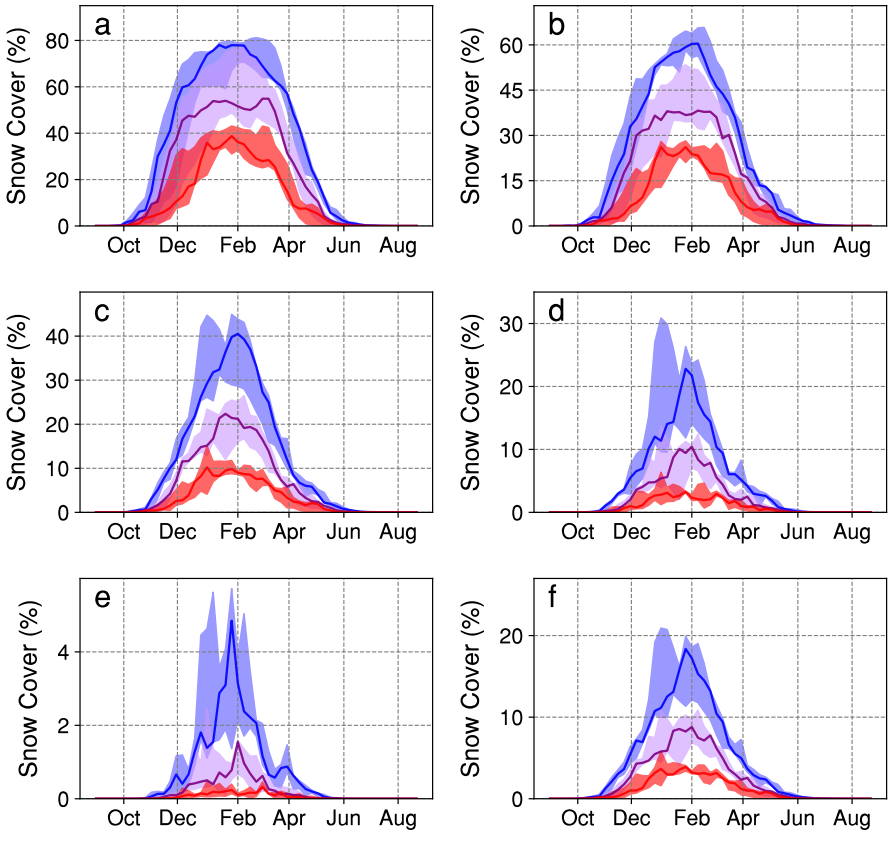

Figure 7. Annual cycles of snow cover (in %) in the three GCM-driven experiments under the historical (blue, 1976-2005), RCP4.5 (purple, 2071-2100) and RCP8.5 (red, 2071-2100) scenarios, at various elevations ranges within our study area: (a) > 3500m, (b) 3000-3500m, (c) 2500-3000m, (d) 2000-2500m, (e) 1500-2000m and (f) whole area. Solid lines represent the three-model medians and the shading corresponds to the three-model spreads.

https://doi.org/10.5194/hess-2020-622
Preprint. Discussion started: 18 December 2020

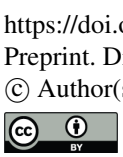

Hydrology and Earth System Sciences
Discussions
Open Access
EGU

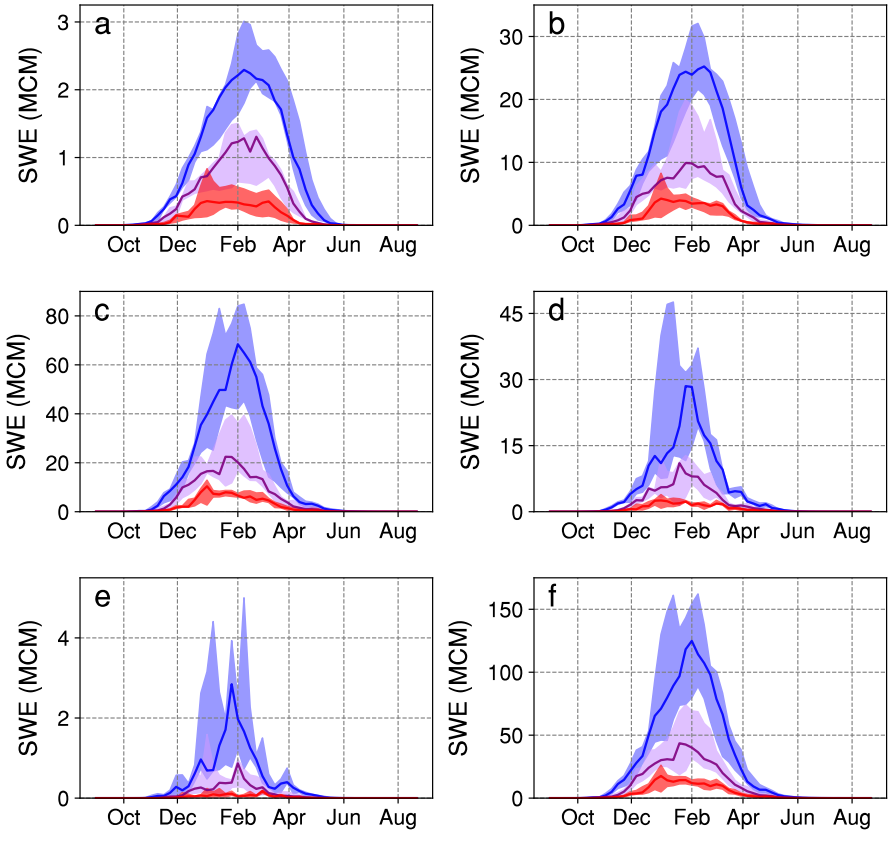

Figure 8. Same as Fig. 7, but for average snow water equivalent (mm, left-hand axis) and corresponding total snow water content (million m3, MCM).

https://doi.org/10.5194/hess-2020-622
Preprint. Discussion started: 18 December 2020

Hydrology and Earth System Sciences
Discussions
Open Access
EGU

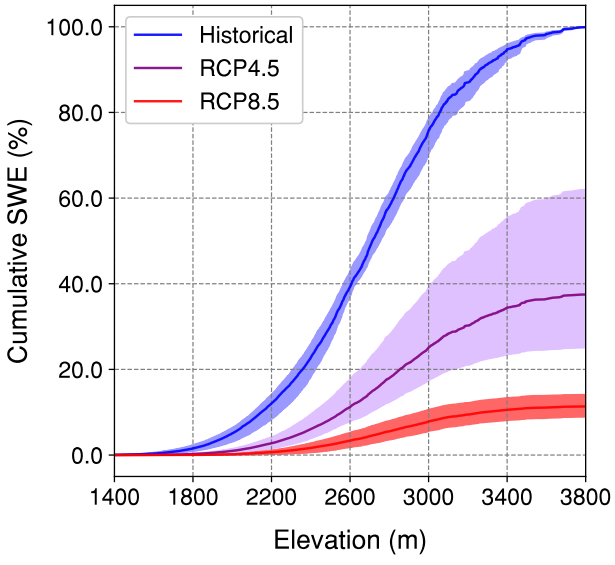

Figure 9. Distribution of cumulative basin-wide SWE with elevation in the GCM-driven experiments, under the historical (black), RCP4.5 (purple) and RCP8.5 (red) scenarios. SWE is normalized in each model by that model?s historical total basin-wide SWE.

https://doi.org/10.5194/hess-2020-622
Preprint. Discussion started: 18 December 2020

Hydrology and Earth System Sciences
Discussions
Open Access
EGU

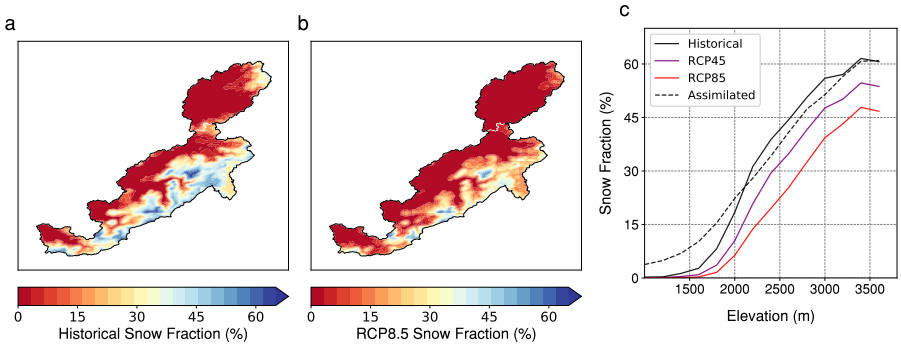

Figure 10. (a-b) Snow fraction of annual precipitation in the (a) historical and (b) RCP8.5 scenario (average between all three GCM-driven simulations). (c) Snow fraction of annual precipitation as a function of elevation, in each scenario (historical, RCP4.5 and RCP8.5; three-model average) and in the assimilated control simulation of T20a.

https://doi.org/10.5194/hess-2020-622
Preprint. Discussion started: 18 December 2020

Hydrology and Earth System Sciences
Discussions
Open Access
EGU

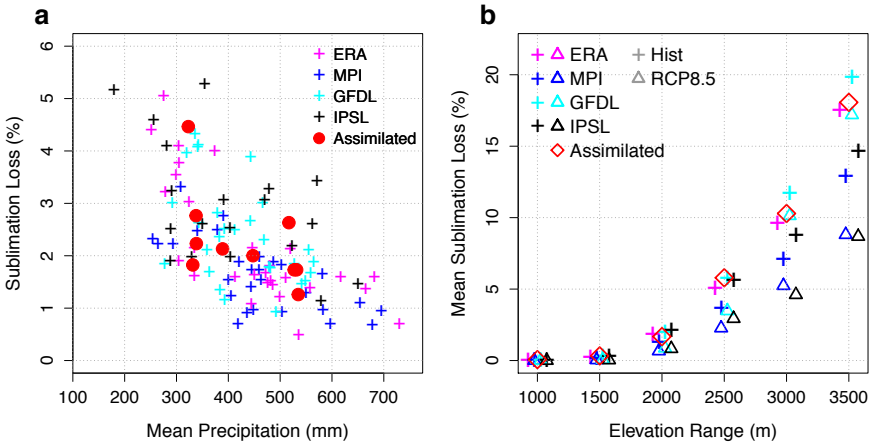

Figure 11. (a) Fraction of annual precipitation lost by sublimation against total annual precipitation in the MRCM downscaled experiments forced with ERA-Interim (1982-2011, magenta), the three GCMs (1976-2005): MPI-ESM-MR (blue), GFDL-ESM2M (cyan) and IPSL-CM5A-LR (black), and the assimilated snow run forced with MODIS and TRMM data only (red, data from T20a). (b) Fraction of annual precipitation lost by sublimation as a function of altitude range in our study area, for the assimilated run from T20a and in the various downscaled experiments, for historical (1976-2005, "+") and RCP8.5 (2071-2100, "Δ") scenarios.

https://doi.org/10.5194/hess-2020-622
Preprint. Discussion started: 18 December 2020

Hydrology and Earth System Sciences
Discussions
Open Access
EGU

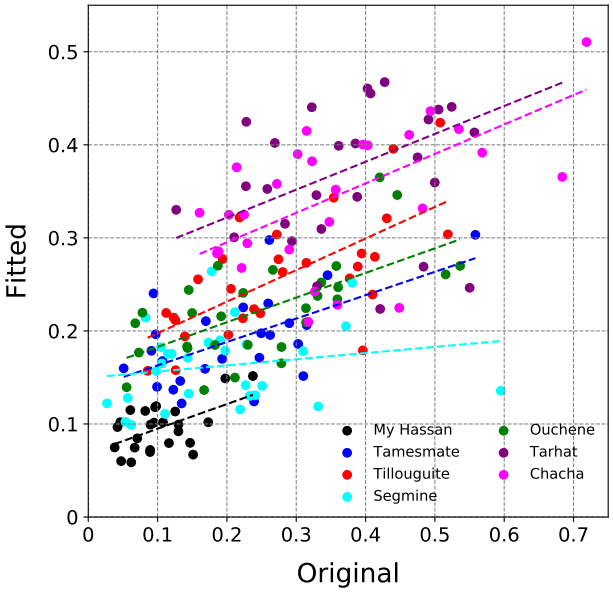

Figure 12. Fitted runoff coefficient values against observed values (defined with TRMM precipitation), for the seven catchments in our study area. Best-fit linear regression lines are shown by dashed lines.

https://doi.org/10.5194/hess-2020-622
Preprint. Discussion started: 18 December 2020

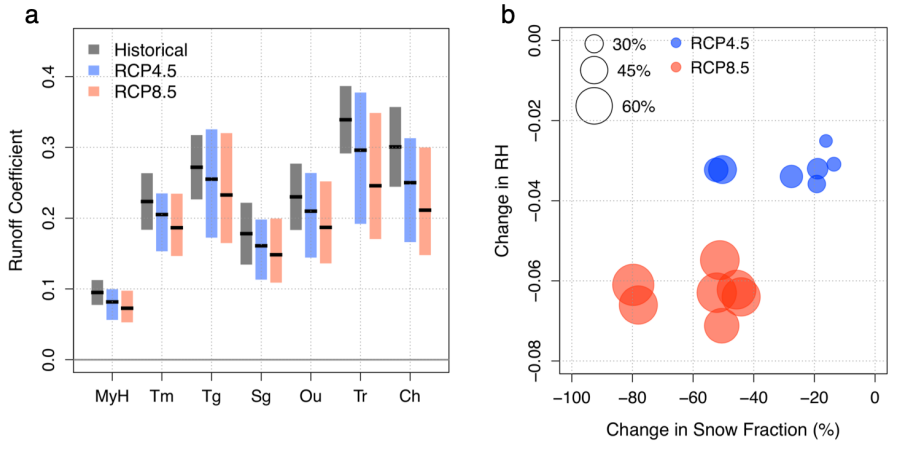

Figure 13. (a) Average runoff coefficients for the seven catchments in the observations (black), and projected average values in the RCP4.5 (blue) and RCP8.5 (red) scenarios. Boxes rep- resent 90% confidence intervals. (b) Projected relative changes in runoff across the seven catchments against relative change in snow fraction (x-axis) and change in catchment-wide relative humidity (y-axis), for the RCP4.5 (blue) and RCP8.5 (red) scenarios.

https://doi.org/10.5194/hess-2020-622
Preprint. Discussion started: 18 December 2020

Hydrology and Earth System Sciences
Discussions
Open Access
EGU

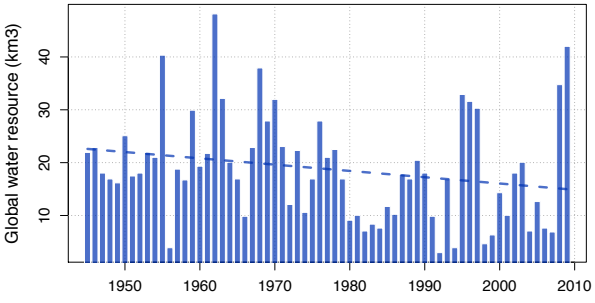

Figure A1. Annual water resources (km^3) in Morocco, 1945-2009. Source: Direction de la Recherche et de la Planification de l'Eau, Rabat. A linear regression fit is shown by the dashed line (p-value: 0.07).